



The PDF files  
contained in this volume are to be published in future  
issues of the journal.  
Please be aware that during the production process  
errors may be discovered which could affect the  
content.  
All legal disclaimers that apply to the journal pertain.

---

**Submitted:** June 6<sup>th</sup>, 2015 – **Accepted:** November 24<sup>th</sup>, 2015

To link and cite this article:

**doi: 10.5710/AMGH.24.11.2015.2921**

PLEASE SCROLL DOWN FOR ARTICLE

---

A solid teal-colored horizontal bar spanning the width of the page at the bottom.

1 **NEW INSIGHTS ON THE *ARISTONECTES PARVIDENS* (PLESIOSAURIA,**  
2 **ELASMOSAURIDAE) HOLOTYPE: NEWS ON AN OLD SPECIMEN**

3 JOSÉ P. O'GORMAN<sup>1,2</sup>

4 <sup>1</sup>División Paleontología Vertebrados, Museo de La Plata, Universidad Nacional de La  
5 Plata, Paseo del Bosque s/n., B1900FWA, La Plata, Argentina.

6 <sup>2</sup>CONICET: Consejo Nacional de Investigaciones Científicas y Técnicas, Argentina.

7 [joseogorman@fcnym.unlp.edu.ar](mailto:joseogorman@fcnym.unlp.edu.ar).

8 28 pag. (text + references); 11 figs; 5 tables

9 Header: NEW INSIGHTS ON THE *ARISTONECTES PARVIDENS* HOLOTYPE

10 CORRESPONDING AUTHOR O'Gorman, José Patricio

11  
12  
13  
14  
15  
16  
17  
18  
19  
20  
21  
22  
23  
24  
25  
26  
27  
28  
29  
30  
31  
32  
33

34 **Abstract.** Additional preparation of the holotype of the Maastrichtian aristonectine  
35 elasmosaurid *Aristonectes parvidens* Cabrera from Chubut Province, Argentina, permits  
36 new observations and reveals features that were not previously described and allows new  
37 interpretations of those that were previously described. Quantitative comparison with non  
38 aristonectine elasmosaurids shows that the increase in the number of alveoli in the  
39 premaxilla, maxilla and mandible is not a consequence of increase in skull size increase.  
40 Instead, decrease in alveolar size and interalveolar space, compared with that seen in non-  
41 aristonectine elasmosaurids, is at least as important. Increase in skull length compared with  
42 non-aristonectine elasmosaurids is not as marked as classically considered: skull length is  
43 equivalent to the length of the first 8–10 cervical vertebrae in non-aristonectines and the  
44 first 10–12 in aristonectines. The ratio of atlas-axis complex length to skull length shows no  
45 significant difference between aristonectine and non-aristonectine elasmosaurids. An  
46 aristonectine autapomorphy not mentioned previously is the decrease in premaxilla  
47 anteroposterior length. This may be correlated with the shortening of the mandibular  
48 symphysis. The cervical region is characterised by a rapid increase in the BI index of the  
49 vertebral centra, indicating a reduction in lateral mobility of the neck. Increase in alveoli  
50 number is achieved as a result of a number of changes that seem to indicate the importance  
51 of the biological role of the length of the alveolar row and mouth aperture. These are  
52 probably related to change in prey size and capture strategy compared with that of non-  
53 aristonectine elasmosaurids, such as a change to smaller fishes or invertebrates and/or a  
54 change from ambushing one prey individual to ambushing multiple simultaneous prey  
55 individuals.

56 **Keywords.** *Aristonectes parvidens*. Aristonectinae. Elasmosauridae. Late Cretaceous

57

58 **Resumen.** NUEVAS OBSERVACIONES SOBRE EL HOLOTIPO DE *ARISTONECTES*  
59 *PARVIDENS* (PLESIOSAURIA, ELASMOSAURIDAE), NOVEDADES SOBRE UN  
60 ANTIGUO ESPÉCIMEN. Nuevas observaciones y una re-preparación del holotipo del  
61 elasmosáurido aristonectino Maastrichtiano *Aristonectes parvidens* Cabrera colectado en la  
62 provincia de Chubut, Argentina, indican características que no se han descrito  
63 anteriormente y permite nuevas interpretaciones de las previamente mencionadas. La  
64 comparación cuantitativa con elasmosauridos no-aristonectinos muestra que el incremento  
65 en el número de alvéolos del premaxilar, maxilar y la mandíbula no es únicamente  
66 consecuencia del aumento de tamaño del cráneo. En su lugar, la disminuciones del tamaño  
67 alveolar y del espacio interalveolar en comparación con aquellos de otros elasmosáuridos  
68 no aristonectinos tienen al menos la misma importancia en el incremento total. El aumento  
69 de la longitud relativa del cráneo en relación a otros elasmosauridos no aristonectinos es  
70 relativamente menos importante que lo considerado clásicamente: longitud cráneo  
71 equivalente a 8-10 primera vértebra cervical (no-aristonectinos) y 10-12 (aristonectinos). El  
72 cociente entre la longitud del cráneo y el complejo- atlas axis no muestra diferencias entre  
73 aristonectinos y no aristonectinos. Una autapomorfía de los aristonectinos previamente no  
74 mencionada es la disminución de la longitud anteroposterior del premaxilar que  
75 posiblemente está correlacionada con el acortamiento de la sínfisis mandibular. La región  
76 cervical se caracteriza por el rápido aumento del índice BI de los centros vertebrales que  
77 indican la reducción de la movilidad lateral del cuello. El aumento de número de alvéolos  
78 logrado debido a una sumatoria de cambios parecen indicar la importancia de la función  
79 biológica del incremento de la longitud de la hilera dentaria, lo que probablemente están  
80 relacionados con un cambio de tamaño de la presa y/o de la estrategia de captura en  
81 comparación con la de los elasmosáuridos no aristonectinos, tales como un cambio a peces

82 más pequeños o invertebrados y/o un cambio de una estrategia de emboscada a captura de  
83 presas múltiples y simultáneas.

84 **Palabras clave.** *Aristonectes parvidens*. Elasmosauridae. Aristonectinae. Cretácico Tardío.

85 ARISTONECTINES are bizarre elasmosaurids that flourished in the last part of the Cretaceous  
86 (Gasparini *et al.*, 2003; O'Gorman *et al.*, 2013, 2014; Otero *et al.*, 2014) and they only  
87 achieved a distribution restricted to the Weddellian Biogeographical Province ( i.e.  
88 Patagonia, Western Antarctica and New Zealand ) and Angola (Cruickshank and Fordyce,  
89 2002; Gasparini *et al.* 2003; O'Gorman *et al.*, 2013; Otero *et al.*, 2014; Araujo *et al.*, 2015).  
90 One of the most important results to come from research on the Late Cretaceous plesiosaurs  
91 from the Weddellian Province is the inference of the elasmosaurian affinities of the  
92 aristonectines (*Aristonectes* Cabrera, 1941; *Kaiwhekea* Cruickshank and Fordyce, 2002), a  
93 topic discussed for the previous 70 years (Cabrera, 1941; Welles, 1962; Cruickshank and  
94 Fordyce, 2002; Gasparini *et al.*, 2003; Benson and Druckenmiller, 2014; Otero *et al.*,  
95 2014). The aristonectines remained poorly known until the recent recognition of *Kaiwhekea*  
96 *katiki* Cruickshank and Fordyce, 2002 as an aristonectine (Ketchum and Benson, 2011;  
97 Otero *et al.*, 2012), the description of the new aristonectine species, *Aristonectes*  
98 *quiriquinensis* Otero, Soto-Acuña, O'Keefe, O'Gorman, Stinnesbeck, Suárez, Rubilar-  
99 Rogers, Quinzio-Sinn, Salazar, 2014 from the upper Maastrichtian of central Chile, and the  
100 recognition of new and previously misinterpreted aristonectine records (O'Gorman *et al.*,  
101 2013; 2014a, b) that have added information about the anatomy and distribution of these  
102 elasmosaurids. However, despite these new results, the internal phylogenetic relationships  
103 among the aristonectines are poorly understood (Otero *et al.*, 2014; O'Gorman *et al.*, 2015).  
104         New preparation of the *Aristonectes* holotype (MLP 40-I-14-6; MLP: *Museo de La*  
105 *Plata*, Buenos Aires Province, Argentina) and the subsequent increases of knowledge about  
106 its anatomy shows new features previously unknown or not completely discussed about  
107 this historical and systematically relevant specimen and allows to see the aristonectine  
108 classical features under a new light. Additionally two explanation about how the

109 aristonectine cranium accommodate the increases number of teeth are tested and a possible  
110 correlation between the skull and neck features of the aristonectines is proposed.

### 111 ***Historical Background***

112 The holotype of *Aristonectes parvidens* (MLP 40-XI-14-6) was collected from Cañadón del  
113 Loro, near Paso del Sapo locality, Chubut Province (Fig. 1.3) by Cristian S. Petersen with  
114 the collaboration of a local resident, Victor Saldivia. The specimen was sent to the *Museo*  
115 *de La Plata* (Buenos Aires Province, Argentina) by Pablo Groeber during September of  
116 1940 as a donation of the *Dirección de Minas y Geología del Ministerio de Agricultura*  
117 (Cabrera, 1941). The identification of the material followed only after the preparation of  
118 the cranium and mandible by Lorenzo Parodi. An incomplete vertebra and phalanges from  
119 the same area had been previously donated to the *Museo de La Plata* (MLP) by Mario  
120 Reguiló and carried to the MLP by Dr. Joaquin Frenguelli. These were later added to the  
121 holotype because, as was mentioned by Cabrera, (1941) they probably belonged to the  
122 same specimen. The MLP 40-XI-14-6 was described by Ángel Cabrera, reconstructed with  
123 plaster and mounted for exhibition (Fig. 1.1; 2.1, 2). The features of *Aristonectes* have  
124 generated doubts about its affinities since the first description and throughout the 20<sup>th</sup>  
125 century (Welles, 1962; Pearsson, 1963; Brown, 1981). Two parts of the specimen were  
126 later re-prepared: the skull and the atlas-axis complex, in order to show more sutures and  
127 alveoli for the revision of Gasparini *et al.* (2003), and the caudal vertebrae, for the revision  
128 by O'Gorman (2013). Both preparations were carried out by the fossil preparator Lic.  
129 Javier Posik.

130 ***Institutional Abbreviations.*** ANSP, Academy of Natural Sciences of Drexel University,  
131 Philadelphia, USA; CIT, California Institute of Technology, Pasadena now in the Natural  
132 History Museum of Los Angeles County; CM, Canterbury Museum, Christchurch, New

133 Zealand; **DMNH**, Denver Museum of Natural History, Denver County, USA; **GNS**,  
134 Institute of Geological and Nuclear Sciences, Lower Hutt, New Zealand; **MACN**, Museo  
135 Argentino de Ciencias Naturales Bernardino Rivadavia, Ciudad Autónoma de Buenos  
136 Aires, Argentina; **MLP**, Museo de La Plata, Buenos Aires Province, Argentina; **OU**, Otago  
137 Museum, Dunedin, New Zealand; **SMU SMO**, Southern Methodist University, Shuler  
138 Museum of Paleontology, Dallas. University of California Paleontological Museum,  
139 California University, San Francisco, USA; **TTU P**, Museum of Texas Tech University,  
140 Lubbock, Texas, U.S.A; **TMP**, Royal Tyrrell Museum of Palaeontology, Drumheller,  
141 Alberta, Canada; **UNSM**, University of Nebraska State Museum, Lincoln, USA.

142 *Anatomical Abbreviations.* **an**, angular; **ana**, atlas neural arch; **aplp**, atlas posterolateral  
143 process; **ar**, articular; **atc**, atlas centrum; **athip**, atlas hipocentrum; **axna**, axis neural arch;  
144 **axc**, axis centrum; **axr**, axis rib; **cr**, cervical rib; **de**, dentary, **dt I**, distal tarsal I; **dt II+III**,  
145 distal tarsal, 2+3; **hf**, hemal facet; **in**, internal nares; **j**, jugal; **lk**, lateral keel; **kl**, keel; **met**  
146 **V**, metatarsal V; **mx**, maxilla; **nc**, neural canal; **pa**, palatine; **par**, parapophyses; **pf**,  
147 pedicellar facet; **pmx**, premaxilla; **poz**, postzygapophyses, **pt**, pterygoid; **q**, quadrate; **sa**,  
148 surangular; **sp**, splenial; **sq**, scamosal; **ti**, tibiale; **vf**, ventral foramina; **vk**, ventral keel; **vn**,  
149 ventral notch; **v**, vomers.

## 150 **MATERIAL AND METHODS**

151 The linear measurements were taken using an electronic calliper that allows  
152 accuracy of 0.01 mm. The indices considered in the description are those proposed by  
153 Welles (1952), which take into account the centrum length (L), the ratio between height (H)  
154 and length of the centrum ( $100 \cdot H/L$ ), and the ratio between breadth (B) and length of the  
155 centrum ( $100 \cdot B/L$ ). In addition, the ratio between the breadth and height ( $100 \cdot B/H$ ) was  
156 considered. In this work both breadth and height were measured on the posterior articular



157 face. The vertebral length index [ $VLI = L/(0.5*(H+B))$ ] was also considered. In order to  
158 test the hypothesis about the relationship between the number of alveoli and the skull  
159 length, the ratio (Ar) between the cranium length (from rostrum tip to occipital condyle=  
160 Cl) and the number of mandibular alveoli (Al) of several elasmosaurids (Table 1) was  
161 calculated as the alveolar ratio ( $Ar = Al/Cl$ ). The Ar value (for each considered  
162 elasmosaurid) \*CL (*Aristonectes parvidens*; *Kaiwhekea katiki*) was used to calculate  
163 increases in alveoli number that is explained only by the increase in the cranial and  
164 mandibular size. The nomenclature used for alveoli measurements follows Smith (2003:  
165 fig. 7; see Fig. 7.1). Particularly the mesodistal measurement was considered used to  
166 compare alveolar sizes. Two ratios were used to compare the ratio between the cranium and  
167 the cervical region of the aristonectine and non-aristonectine elasmosaurids: 1] the ratio  
168 between the cranium length (Cl) and atlas-axis complex length and 2] the number of  
169 cervical vertebrae from the atlas that form a neck sector as long as the cranium length (Cl).

## 170 SYSTEMATIC PALEONTOLOGY

171 Subclass SAUROPTERYGIA Owen, 1860

172 Order PLESIOSAURIA de Blainville, 1835

173 Superfamily PLESIOSAUROIDEA Welles, 1943

174 Family ELASMOSAURIDAE Cope, 1869

175 Subfamily ARISTONECTINAE O'Keefe and Street, 2009 (sensu Otero *et al.*, 2012)

176 Genus *Aristonectes* Cabrera, 1941

177 **Type Species.** *Aristonectes parvidens* Cabrera, 1941.

178 **Emended Diagnosis.** (modified from Gasparini *et al.*, 2003; Otero *et al.*, 2014).

179 Aristonectine elasmosaurid with large, an at least slightly flattened and broad skull without  
180 premaxillary–maxillary constriction, which differs from the high skull of *Kaiwhekea katiki*;

181 gracile mandible with very short symphysis; homodont dentition with more than 50  
182 mandibular procumbent alveoli; anterior and middle cervical vertebrae with low average  
183 VLI (~80), but slightly higher than those of *Kaiwhekea katiki*. Additional features showing  
184 differences between *Aristonectes* and *Kaiwhekea*, although they are not found/ in all of the  
185 representative skulls: 13 premaxillary teeth (not preserved in *A. quiriquinensis*), differing  
186 from the seven premaxillary teeth of *Kaiwhekea*; 50 or more teeth in the maxilla (not found  
187 in *A. quiriquinensis*), differing from the 36 teeth recorded in *Kaiwhekea*.

188 *Aristonectes parvidens* Cabrera, 1941

189 Figs. 2; 3; 4.1; 8; 9.1,2; 10, 1–9; 11. 1–9

190 **Type material.** MLP 40-XI-14-6, part of a skull attached to the mandible, atlas-axis  
191 complex, anterior and middle cervical vertebrae, anterior caudal vertebrae and one posterior  
192 caudal vertebrae, caudal ribs and an incomplete limb) (Cabrera, 1941: figs 1–6; Gasparini  
193 *et al.*, 2003:figs 1–3).

194 **Type Locality and Horizon.** Cañadón del Loro, middle Chubut River (42° 40" S 70 ° 00"  
195 W), northwestern Chubut Province, Patagonia, Argentina (Cabrera, 1941); Lefipán  
196 Formation, Maastrichtian (Lesta and Ferello, 1972; Page *et al.*, 1990).

197 **Diagnosis.** *Aristonectes* species with symphyseal lingual groove; mandible higher than in  
198 *A. quiriquinensis*, keel on the dorsal surface of the retroarticular process, short projection of  
199 the atlas along the axis rib. Absence of lateral keel independent of the dorsal margin of the  
200 parapophysis.

#### 201 **Description**

202 The specimen MLP 40-XI-14-6 was originally described by Cabrera, 1941 and then  
203 carefully re-described by Gasparini *et al.* (2003). Here, only specific features previously not

204 reported or reinterpreted are described, carefully illustrated and discussed and measurement  
205 (Tables 2, 3) are added.

206 **Alveoli.** The high number of alveoli in the aristonectine skull has been recorded since the  
207 description by Cabrera (1941) who indicated the presence of 15 premaxillary alveoli while  
208 Gasparini *et al.* (2003) indicated a number of 10 to 13. The difference is due to the  
209 different interpretation about where the premaxilla-maxilla suture is located (Fig. 2.6).

210 Careful observation of the specimen and a comparison with *Kaiwheke katiki* indicates the  
211 most probable number of premaxillary alveoli is 13. The number of maxillary teeth  
212 indicated by Cabrera (1941) was 26 whereas Gasparini *et al.* (2003) counted 51–53  
213 maxillary alveoli. The new observations confirm the presence of 37 clearly visible alveoli  
214 and at least 14 inferred by a sulcus on the counterpart in the lower jaw and, therefore, the  
215 presence of at least 51 maxillary alveoli. Cabrera (1941) indicated the presence of 58  
216 mandibular teeth and 60–65 mandible alveoli were observed by Gasparini *et al.* (2003).

217 This revision of the specimen indicates that the number is probably at least 63 but  
218 uncertainty remains and the number could be between 63 and 65. Additionally, the lateral  
219 inclination of the alveoli series is confirmed (Fig. 2.3, 4, 6), a feature mentioned by  
220 Gasparini *et al.* (2003) and recently observed in *A. quiriquinensis* but difficult to determine  
221 in *Kaiwhekea* (Otero *et al.*, 2014; J.P. O'G. pers. obs.).

222 **Internal naris.** Gasparini *et al.* (2003: fig. 3D) did not attempt to identify the elements that  
223 limit the internal naris other than the vomer and the maxilla. O'Gorman (2013) only  
224 mentioned the elements that could participate: vomer, maxilla and palatine but no attempt  
225 at a detailed reconstruction or discussion was made. The preserved elements of the anterior  
226 part of the palate are: premaxilla, anterior half of the vomer, maxilla, palatine and, a  
227 previously not mentioned, anterior part of the pterygoids. One of the problems relating to

228 the anterior structure of the palate is that the suture between the vomer and premaxilla  
229 seems to be asymmetrical, as was figured by Gasparini *et al.* (2003: fig. 3). However,  
230 careful observation indicates that the probable suture is located as shown in figure 3.3, 4.  
231 Unfortunately, the posterior border of the naris is not preserved (although a posterior bone  
232 wall is preserved, it is not clear if it is natural). A comparison between *Aristonectes*  
233 *parvidens* and a non aristonectine elasmosaurid such as *Libonectes morgani* (Welles, 1949)  
234 (Fig. 6.11, 12) indicates that the vomer of *A. parvidens* has two lateral depressions that  
235 limit the vomeronasal fenestra recorded by Gasparini *et al.* (2003), giving a premaxilla-  
236 vomer suture with the premaxilla presenting the “M” shape mentioned by Gasparini *et al.*  
237 (2003) and a long anterior process (Fig. 3.3, 4), features absent in other elasmosaurids  
238 (Carpenter, 1997: fig. 2D; Sato *et al.*, 2006: fig. 4C; Vincent *et al.*, 2011: fig. 2E). The  
239 posteriormost part of the vomer shows an open suture between both lateral vomeral  
240 elements (Fig. 3.1, 3), usually fused or with a strong suture in adults (Carpenter, 1997; Sato  
241 *et al.*, 2006). This open suture is congruent with the only other palate known from an  
242 aristonectine (Chatterjee and Small, 1989: fig. 4), where the vomers are only anteriorly and  
243 medially fused but posteriorly they show a wide intervomerial space generated by the  
244 absence of a medial suture. If the vomer of *Aristonectes* has the same morphology, the  
245 vomer had to expand laterally and generate a relatively small and anterioposteriorly long  
246 internal naris (Fig. 3.4) which differs from the morphology inferred by O’Gorman (2013)  
247 and gives a reconstruction which is more consistent with the morphology observed in other  
248 elasmosaurids (Carpenter, 1997). Another interesting feature of the *Aristonectes parvidens*  
249 holotype regards the probable dorsal overlapping of medial element that projects dorsally  
250 to the vomer. This element was interpreted as part of the vomer by Gasparini *et al.* (2003)  
251 and O’Gorman (2013). However, careful observation shows a possible suture between both

252 elements and, therefore, the dorsal and posterior elements could not be part of the vomer  
253 (Fig. 3.1, 2). By its medial position, this element is possibly the anteriormost part of the  
254 pterygoid that overlaps part of the vomer dorsally and is visible in palatal view due to the  
255 absence of the posterior part of the vomer.

256 **Mandibular symphysis.** The mandibular symphysis of MLP 40-XI-14-6 is short and, as  
257 was mentioned by Otero *et al.* (2014) bears a depression, the “deep groove” of Otero *et al.*  
258 (2014) on its internal surface (Fig. 3.2). The ventral side of the symphysis does not show  
259 the mental boss observed by Otero *et al.* (2014) in the symphysis of *A. quiriquinensis* (Fig.  
260 3.1; 4.1). However, the mandible surface of the holotype of *A. parvidens* has suffered the  
261 loss of the external layer of bone and, therefore, it is possible that at least weak mental boss  
262 was originally present. This is even probable because the mental spines of *A.*  
263 *quiriquinensis* are located in the lateral margins of a wide symphyseal sulcus, which is  
264 present in *A. parvidens* (Fig. 4.1). Comparison between the ventral surface of the  
265 symphysis of *A. parvidens* and those of non aristonectine elasmosaurids (Fig. 4.1–4) shows  
266 that they share the symphyseal sulcus but that of *Aristonectes parvidens* is much wider,  
267 following the general widening of the symphysis. Another interesting feature of the  
268 symphysis is the reduced symphyseal post alveolar surface similar to that observed on *A.*  
269 *quiriquinensis* but different from other elasmosaurids (Carpenter, 1997:fig. 2E). All this  
270 corroborates the observations of Gasparini *et al.* (2003) and Otero *et al.* (2014) about the  
271 presence of a relatively weak symphysis compare to non-aristonectine elasmosaurids (Fig,  
272 5.1–4).

273 **Glenoid cavity, retroarticular process and coronoid process.** Only the right glenoid cavity  
274 and the proximal part of the retroarticular process is preserved. The glenoid cavity is deep  
275 (42 mm antero-posterior length in dorsal view; 32 mm dorsoventral length) and strongly

276 posteromedially directed (Fig. 4.5, 6). As Otero *et al.* (2014) mentioned, a marked keel  
277 projects from the tip of the reotroarticular process process to the limit to the posterior limit  
278 of the glenoyd cavity (Fig. 4.5, 6). The medial view of the right mandible (Fig. 3.5) shows a  
279 relatively high and rounded coronoid and additionally it is observed the suture between the  
280 angular and surangular and splenial remains open.

281 ***Atlas-axis complex.*** The atlas axis was carefully described by Gasparini *et al.* (2003). The  
282 description focused on the elements that formed it and its distribution. Here, other features  
283 that appear distinctive among elasmosaurids are recorded and shown in figures. Three main  
284 features of the atlas-axis of *Aristonectes parvidens* are: the presence of open sutures, the  
285 absence of a developed ventral keel and the circular anterior atlantal cup. The presence of  
286 open sutures is quite interesting, as sutures are usually fully closed in the atlas-axis of adult  
287 elasmosaurids (Wiffen and Moisley, 1986; Carpenter, 1999; Kubo *et al.*, 2012; Sachs and  
288 Kear, 2014; O'Gorman *et al.*, 2015). Although part of this phenomenon could be  
289 consequence of the preparation, it seems to be at least partially natural feature (Fig 8.1, 2),  
290 probably connected to some difference in the relative time of suture closure among  
291 elasmosaurids. The second mentioned feature, the absence of a developed ventral keel (Fig.  
292 8.6) is unusual among elasmosaurids (Welles, 1943; Kubo *et al.*, 2012; O'Gorman *et al.*,  
293 2015; Sachs and Kear, 2014) but it seems to be present in *Tuarangisaurus keyesi* (Wiffen  
294 and Moisley, 1986). Finally, the presence of a circular atlantal cup (Fig. 7.4) is also unusual  
295 among elasmosaurids, in which they are usually higher than broad (Fig. 9). Another feature  
296 recorded for atlas-axis of *A. parvidens* is the absence of ventral foramina (Fig. 8.6), which  
297 are present in some other elasmosaurids (Sachs and Kear, 2014; O'Gorman *et al.*, 2015).  
298 Also, the postzygapophysis of the axis appears to be ventrally projected in the figure of  
299 Cabrera (1941: fig. 2B) and Gasparini *et al.* (2003: fig. 2A, 3E). Detailed observation

300 revealed that the observed “ventral projection” (Fig. 8.1, 2, 5) is part prezygapophysis of the  
301 third vertebra which remains attached to the postzygapophysis of the atlas-axis complex  
302 and, therefore, it is not a natural feature. Finally the posterolateral process of the atlas  
303 seems to be broken in its distalmost part (Fig. 8. 4) although it was probably not as long as  
304 that recorded for *A. quiriquinensis* (Otero *et al.*, 2014).

305 **Lateral keel.** The holotype preserves a cervical series that belong to the anterior part of the  
306 neck (Fig. 9.1). This was described by Gasparini *et al.* (2003) but the question of the lateral  
307 keel needs some clarification. In the original description Cabrera (1941) did not record or  
308 include figures of any lateral keel in the cervical vertebrae of the holotype (Cabrera, 1941:  
309 figs 3, 4). Afterwards Gasparini *et al.* (2003) described “scarcely visible lateral crests that  
310 can occur only on a single side”. The present revision indicate tha the only constant  
311 convexity observed in the cervical vertebrae of MLP 40-XI-14-6 is a distinctive convex  
312 area located above the parapophysis (Fig. 10.2, 8) which is evident in the specimen because  
313 the cervical ribs are displaced. However, the dorsal margin of the parapophysis seems to be  
314 more prominent than in other elasmosaurids (see Fig 10.10 of non elasmosaurid specimens,  
315 CIT 2832, referred to *Afrosaurus furlongi* by Welles, 1943). It is likely that the dorsal  
316 margin of the parapophysis, together with the capitulum of the cervical rib, has produced an  
317 even larger convex zone. Therefore, direct observation of the holotype indicates that there  
318 are not well developed lateral keels independent of the dorsal margin of the parapophyses.  
319 Another possibility is that a faint lateral ridge was erased during the original preparation,  
320 but there is no way to test this.

321 **Caudal centra.** Cabrera (1941) indicated that only two caudal vertebrae were preserved.  
322 These are indeed caudal vertebrae but Cabrera misidentified eight caudal vertebrae as  
323 posterior cervicals and was later corrected by Gasparini *et al.* (2003) , Figure 11.1–4.

324 Cabrera did not mention any ventral foramina in his “posterior cervicals”=caudals and  
325 neither did Gasparini *et al.*, (2003). Additional preparation shows the presence of at least  
326 five ventral foramina in one vertebra (Fig. 11.3). This is very surprising considering that  
327 one vertebral foramen (or two in anteriormost caudals) is the most frequent number of  
328 foramina among elasmosaurids (Benson and Druckenmiller, 2014) and the presence of five  
329 large and well defined ventral foramina has been recorded only for the specimen considered  
330 here. Another interesting feature of the caudal vertebrae is their proportions. The figure  
331 11.10 compares the HI and BI indexes of the caudal vertebrae of MLP 40-XI-14-6 and non  
332 aristonectine elasmosaurids. The comparison shows that the caudals of MLP 40-XI-14-6  
333 show relatively high HI and BI indexes.

334 **Caudal ribs.** No caudal ribs were described by Cabrera (1941), probably because they were  
335 wrongly identified. Gasparini *et al.* (2003) failed to mention them as well. However, in  
336 the material, there are several damaged caudal ribs similar to the caudal ribs of other  
337 elasmosaurid (J.P.O’G. per. obs) but with a slightly larger proximal expansion in the  
338 capitulum (Fig. 11.6, 7), related to the large parapophysis of the caudal vertebrae (Fig.  
339 11.2).

340 **Limb.** The only preserved limb elements of MLP 40-XI-14-6 were reconstructed by  
341 Cabrera (1941) as part of only one paddle but he stated that he was not certain that all the  
342 elements belonged to the same limb. Therefore, the dimensions are not adequate to  
343 calculate aspect ratios. The proximal limb elements were arranged in different ways by  
344 different authors. Figures 11.8 and 11.9 show the original interpretation of Cabrera (1941)  
345 and the ones of O’Gorman (2013) and Otero *et al.* (2014) respectively. The interpretation of  
346 the elements given here follows the last of these.

#### 347 **CALCULATIONS**



348 **Correlation between mandibular alveoli and skull size.**

349 Table 4 shows the cranial lengths (from premaxilla tip to occipital condyle) of six  
350 elasmosaurids and the ratio number of mandibular alveoli/cranium length (alveolar  
351 rate=Ar). For calculation *Tuarangisaurus* (20 alveoli); *Aristonectes* (64 alveoli) and  
352 *Kaiwhekea* (43 alveoli) were considered. The last column “predicts” the alveoli number of  
353 a non-aristonectine elasmosaurid if it had an aristonectine-like cranium size (non-  
354 aristonectine mandibular alveoli number/non-aristonectine cranium length) \* aristonectine  
355 cranium length. This column shows that the increase in length of the skull of aristonectine  
356 only partly “explains” the increases of alveoli number (between 21 and 34 for *Aristonectes*  
357 *parvidens* and 18 and 30 for *Kaiwhekea katiki*).

358 **Alveoli size**

359 In order to test the hypothesis of the relatively small alveoli of *Aristonectes*  
360 *parvidens* compared with non-aristonectine elasmosaurids, the meso-distal measurements  
361 of the alveoli of MLP 40-I-14-6 were recorded and are plotted in Figure 7.2. Additionally,  
362 Figure 7.2 plots the alveoli size of *Tuarangisaurus keyesi* Wiffen and Moisley, 1986, a non-  
363 aristonectine elasmosaurid from the Campanian–Maastrichtian of New Zealand in order to  
364 compare them with those of *Aristonectes parvidens*. The comparison of both alveolar  
365 series shows a marked difference in mesodistal length of the alveoli.

366 **Skull/neck proportion**

367 Table 5 shows the ratio between the cranium length (from premaxilla tip to occipital  
368 condyle ) and the atlas-axis complex length. It indicates that the values for *Aristonectes*  
369 falls within the range of values calculated for other elasmosaurids.

370 **DISCUSSION AND CONCLUSION**

371 *Alveoli number and size*. The recognition of the elasmosaurid affinities of aristonectines  
372 raised the question about how this group achieved its classically mentioned distinctive  
373 features among elasmosaurids, such as the relatively large skull, high number of alveoli and  
374 short neck. The question about of how an elasmosaurid skull could accommodate increase  
375 in the number of alveoli, is a relevant issue that has not been previously discussed. The  
376 number of alveoli among non-aristonectine elasmosaurids has been largely recognised to be  
377 lower than that of the aristonectines and the same is true for the skull size (Table 4).  
378 However, no attempt to look for some correlation between skull size and alveoli number  
379 was previously undertaken, therefore, it was not discussed if whether the increase in  
380 alveoli number is a direct effect of the increase in cranial size and the retention of teeth size  
381 or if other factors are involved. In order to test this, two analyses were carried out. Table 4  
382 shows the ratio mandibular alveoli number/cranium length. The last column “predicts” the  
383 alveoli number of a non-aristonectine elasmosaurid with an aristonectine-like cranium size.  
384 This column shows that the increase in length of the skull of aristonectines only partly  
385 “explains” the increases of alveoli number (between 21 and 34 for *Aristonectes parvidens*  
386 and 18 and 30 for *Kaiwhekea katiki*). Therefore, the enlarged number of alveoli is only  
387 partially explained by the enlargement of the skull compared with non-aristonectine  
388 elasmosaurids.

389         The previous result indicates that other features, such as the small size of the alveoli  
390 and the absence of large interalveolar spaces and/or diastemata, generate the space for the  
391 additional alveoli. In order to investigate the difference in the alveoli size between  
392 aristonectines and non aristonectine, the meso-distal measurements of the alveoli of MLP  
393 40-I-14-6 were recorded and plotted in Figure 7.2. Additionally, Figure 7.2 includes the  
394 alveoli sizes for *Tuarangisaurus keyesi* Wiffen and Moisley, 1986, a non-aristonectine

395 elasmosaurid. The comparison of both alveolar series shows a marked difference between  
396 the size of the alveoli, indicating that this sizes difference is the second feature that allows  
397 to accommodation of the high alveolar account. Therefore, these two mentioned features  
398 together with the small interalveolar spaces (between 1–2 mm), the ogival shape that  
399 increases the cranial and mandibular alveolar margin, and the absence of diastema generate  
400 the difference in the alveolar count compared with that of non- aristonectine elasmosaurids.

401 **Vomer-ptyergoid contact.** The position of the anteriormost end of the pterygoid overlapping  
402 the vomer has not been previously recorded for elasmosaurids. However a dorsal view of  
403 articulated specimens of these two elements has not been described among elasmosaurids  
404 and therefore it could be a widespread features. A similar condition was discussed by  
405 Schumacher (2008: fig. 2B) and Schumacher *et al.* (2013) for other plesiosaurs such as  
406 *Megacephalosaurus eulerti* Schumacher, Carpenter and Everhart, 2013 and  
407 *Dolichorhynchops osborni* Williston, 1903 and the idea that this is a widespread feature  
408 among Plesiosauria was pointed out because, as was mentioned by Schumacher (2008) and  
409 Schumacher *et al.* (2013), the common two-dimensional observation in palate view does  
410 not negate the possible overlapping of the vomer with anterior extensions of the pterygoids  
411 in different plesiosaur taxa. The presence of this feature in the elasmosaurid *Aristonectes*  
412 *parvidens*, a highly derived elasmosaurid, reinforces the idea that this could be a usual  
413 feature among Plesiosauria.

414 **Cranial proportions.** Skull proportions of *Aristonectes* have been previously mentioned as  
415 low and ogival shaped. This is produced partially by the increase in transverse width near  
416 the rostrum and mandibular symphysis. Additionally, the holotype of *A. parvidens* shows  
417 another interesting feature which was not previously mentioned and is shared with  
418 *Kaiwehekea*: the low ratio between premaxilla and maxilla anteroposterior length. This is

419 evident when the cranial proportions are compared among aristonectine and non-  
420 aristonectines (Figure 5.7–10). The same proportion is observed in palatal view (Fig. 5.5,  
421 6). Therefore, the relatively shorter premaxilla appears to be a feature of the aristonectines.  
422 Additionally, a short mandibular symphysis is also present, a feature known since the  
423 original description of Cabrera (1941; see Fig. 5.1–4). It is interesting that both the  
424 anteroposterior length of the premaxilla and the length of the symphysis show both a  
425 shortening. The functional reason for this correlation is currently unknown.

426 ***Large cranium or large body?: skull/ cervical vertebrae proportions.*** Another feature also  
427 cited since Cabrera (1941) for *Aristonectes* is the large skull. It is clear that among the  
428 distinctive small skulled elasmosaurids the aristonectines *Aristonectes parvidens*;  
429 *Aristonectes quiriquinensis* and *Kaiwhekea katiki* stand out with their large skulls (Fig. 6.1,  
430 2). However, the relationship between skull size and vertebral length has not been  
431 previously considered. Figure 6.1 indicates that the skull is as long as the sum of the  
432 lengths of the first eleven to twelve cervical vertebrae. Similar values are recorded for  
433 *Kaiwhekea* (~10 to 11) but other elasmosaurids show slightly lower values. Therefore,  
434 although the skull is relatively larger than in other elasmosaurids, the difference is not as  
435 big as was classically pointed out. The ratio between the skull length and the atlas-axis  
436 length (Tab. 5) shows that this is even among the ratio of other elasmosaurids.

437 ***The problem of the lateral keel.*** The apparent absence of a lateral keel on the cervical  
438 vertebrae of MLP 40-XI-14-6 is surprising because it is a typical elasmosaurid feature. The  
439 only constant convexity observed in the cervical vertebrae of the specimen is a distinctive  
440 convex area located above the parapophysis (Fig. 10.2, 8) which is more evident in the  
441 specimen because the cervical ribs are displaced. However, the dorsal margin of the  
442 parapophysis seems to be more prominent than in other elasmosaurids (see Fig 10.10 of

443 non elasmosaurid specimens, CIT 2832, referred to *Afrosaurus furlong* by Welles, 1943). It  
444 is evident that the dorsal margin of the parapophysis, together with the capitulum of the  
445 cervical rib, produced an even larger convex zone. Therefore, direct observation of the  
446 holotype indicates that there are no well developed lateral keels independent of the dorsal  
447 margin of the parapophysis. The other preserved aristonectines also show complex patterns  
448 of features regarding the lateral margins of their cervical vertebrae. *Kaiwhekea* was  
449 described as lacking a lateral ridge (Cruickshank and Fordyce, 2002) and a personal  
450 observation of the holotype also failed to record this feature. On the other hand, *A.*  
451 *quiriquinensis* shows lateral keel. Juvenile aristonectine specimens show a convex area  
452 dorsal to the parapophysis called “lateral keel” but not a completely independent distinctive  
453 lateral keel (Chatterjee and Small, 1989: fig.10D; Otero *et al.*, 2012: fig. 3C, D). Therefore,  
454 more complete and well prepared specimens are necessary to answer the question about the  
455 nature and distribution of the lateral keel among aristonectines.

456 **Cervical ribs.** Some of the cervical vertebrae preserve the cervical ribs attached, although  
457 most are displaced (Fig. 10.2, 5). A comparison between the cervical ribs of the 9<sup>th</sup> cervical  
458 vertebra of *Aristonectes parvidens* and the 10<sup>th</sup> of the non aristonectine *Vegasaurus molyi*  
459 O’Gorman, Salgado Olivero and Marensi, 2015 indicates that the cervical ribs of  
460 *Aristonectes* were probably relatively longer and wider than those of the non aristonectine.

461 **Skull and neck features: integrated interpretation.** Aristonectines show several  
462 features that indicate marked differences with other elasmosaurids. The comparisons based  
463 on *A. parvidens* carried out in this contribution confirm and improve our knowledge about  
464 these differences. The analysis of the alveolar number seems to indicate that the large  
465 number of alveoli of *Aristonectes parvidens* was achieved, not only by the absolute and  
466 relative enlargement of the skull (which only partly “explains” the increases in the alveoli

467 number), but also by the small alveolar size and reduced interalveolar spaces. Therefore,  
468 there are at least three ways of accommodating the phylogenetical increases of alveoli  
469 number: increases of skull size, decreases of alveolar size and a reaccommodation  
470 modifications due to diastema elimination and reduction of interalveolar spaces. This could  
471 indicate that the increases of alveoli and the teeth located in them was achieved by a  
472 complex process that involved several factors and, therefore, was probably favoured by the  
473 importance of the biological role of the length of the tooth line and mouth aperture. These  
474 suggest a change of prey and/or strategy of capture, such as moving to smaller fishes or  
475 invertebrates and/or/ changing from ambush one-by-one prey to multiple simultaneous prey  
476 individuals. These conclusions are consistent with the type of prey indirectly inferred for  
477 aristonectines. The exactly prey preference of *Aristonectes parvidens* or any other  
478 aristonectine is not known by direct evidence as the only gut contents are recorded until  
479 now are gastroliths collected associated with a specimen referred to *Aristonectes* sp.  
480 (O'Gorman *et al.*, 2014) and *Aristonectes quiriquinensis* (Otero *et al.*, 2014). However some  
481 inferences have been made based on tooth morphology. Although tooth morphology of  
482 *Aristonectes parvidens* is not known, some teeth of *A. quiriquinensis* were described by  
483 Otero *et al.* (2014: fig. 7B). These show the features described by Massare (1987) for the  
484 tooth crown morphology of the guild "Pierce I": pointed apex, no wear apex, no cutting  
485 edges and shape of preserved tooth (height/basal diameter higher than 3.0). Following  
486 Massare (1987) this type of tooth was used for piercing soft prey items such as small fish  
487 and soft cephalopods. Chatterjee and Small (1989) proposed that the teeth of *Morturneria*  
488 *seymourensis* (considered a junior synonym of *Aristonectes* by Gasparini *et al.*, 2003)  
489 belong to the 'Trap guild', which used its specialized tooth occlusion as a device for  
490 straining and trapping preys such as small fish and crustaceans. A similar prey preference

491 was proposed by Cruickshank and Fordyce, 2002 (*K. katiki*) and Gaspaini et al., 2003 (*A.*  
492 *parvidens*). This inference seems to be correlated with the features of the skull and neck  
493 previously discussed because a trap strategy could be related to a larger mouth aperture and  
494 an increase in absolute cranium size, which is a feature of the aristonectines. Also the  
495 configuration of skull and neck characters seems to be correlated because large skull used  
496 in ram feeding, requires greater support from the cervical region and the support area is  
497 related to the neck transverse section, therefore, the increases in height and width of the  
498 cervical centra could represent a mechanical necessity. However, increases in width and a  
499 relative increase of height relative to length compared with other elasmosaurids generate a  
500 restriction in the lateral and dorsoventral movements of the neck (Massare and Sperber,  
501 2001). Restriction of the mobility of the posterior part of the neck of elasmosaurids related  
502 to the change of centra proportions and increased height of neural spines has been  
503 suggested by previous authors (Masare and Sperber, 2001; Zamit et al., 2008). The  
504 difference observed for the aristonectines is a major restriction compared with other  
505 elasmosaurids precluding ambush hunting based on quick lateral movement, but give  
506 additional support against the drag forces produced by the large skull. Finally, the absence  
507 of a lateral keel (*Kaiwhekea*) or the absence of an independent lateral keel (*A. parvidens*)  
508 could be related to changes in neck movements.

509         Although these are preliminary conclusions, it seems probable that increases in  
510 skull length increases in the total number of teeth changes in cervical proportions  
511 compared with other elasmosaurids and the type of prey and/or capture strategy were  
512 highly correlated.

513

514 **ACKNOWLEDGEMENTS**

515 Thanks to Ewan Fordyce (Otago University, New Zealand); Paul Scofield  
516 (Canterbury Museum), John Simes (National Paleontology Collection, GNS Science  
517 Avalon, New Zealand) and Maureen Walsh (California Natural History Museum, Dinosaur  
518 Institute) for allowing to review the elasmosaurs from those institutions. Thanks to Paula  
519 Arregui (Universidad Nacional de La Plata) and N. Hiller for improving the English  
520 grammar . This research was supported by PICTO-2010-0093, PIP 0433, UNLP N 607, and  
521 PICT 2012-0748

522

## 523 REFERENCES

- 524 Araújo, R., Polcyn, M.J., Lindgren, J., Jacobs, L.L., Schulp, A.S., Mateus, O., Gonçalves,  
525 A.O., and Morais, M-L. 2015. New aristonectine elasmosaurid plesiosaur specimens  
526 from the Early Maastrichtian of Angola and comments on paedomorphism in  
527 plesiosaurs. *Netherlands Journal of Geosciences-Geologie En Mijnbouw* 94: 93–108.
- 528 Benson, R.B., and Druckenmiller, P.S. 2014. Faunal turnover of marine tetrapods during  
529 the Jurassic–Cretaceous transition. *Biological Reviews* 89: 1–23.
- 530 Brown, D.S. 1981. The English Upper Jurassic Plesiosauroidea (Plesiosauria) and a review of the  
531 phylogeny and classification of the Plesiosauria. *Bulletin of the British Museum*  
532 *(Natural History), Geology* 17: 253–347.
- 533 Cabrera, A. 1941. Un Plesiosaurio nuevo de Cretáceo del Chubut. *Revista del Museo de la*  
534 *Plata (Nueva Serie)* 2: 113–130.
- 535 Carpenter, K. 1997. Comparative cranial anatomy of two North American Cretaceous  
536 plesiosaurs. In: J. M. Callaway and E. L. Nicholls (eds.), *Ancient Marine Reptiles*.  
537 Academic Press, San Diego, p. 191–216.



- 538 Carpenter, K. 1999. Revision of North American elasmosaurs from the Cretaceous of the  
539 Western Interior. *Paludicola* 2: 148–173.
- 540 Chatterjee, S., and Small, B.J. 1989. New plesiosaur from the Upper Cretaceous of  
541 Antarctica. *Special Publications of the Geological Society* 47: 197–215.
- 542 Cruickshank, A.R.I., and Fordyce, R.E. 2002. A new marine reptile (Sauropterygia) from  
543 New Zealand: Further evidence for a Late Cretaceous Austral radiations of  
544 cryptoclidid plesiosaur. *Palaeontology* 45: 557–575.
- 545 Cope, E.D. 1869. Synopsis of the extinct Batrachia, Reptilia and Aves of North America.  
546 *Transaction of the American Philosophical Society* (new series) 14: 1–252.
- 547 Blainville, H.D. de. 1835. Description de quelques espèces de reptiles de la Californie,  
548 précédée de l'analyse d'un système général d'herpetologie et d'amphibiologie.  
549 *Nouvelles Archives du Museum d'Histoire Naturelle* 4: 233–296.
- 550 Gasparini, Z., Bardet, N., Martin, J.E., and Fernandez, M. 2003. The elasmosaurid  
551 plesiosaur *Aristonectes* Cabrera from the Latest Cretaceous of South America and  
552 Antarctica. *Journal of Vertebrate Paleontology* 23: 104–115.
- 553 Ketchum, H.F., and Benson, R.B. 2010. Global interrelationships of Plesiosauria (Reptilia,  
554 Sauropterygia) and the pivotal role of taxon sampling in determining the outcome of  
555 phylogenetic analyses. *Biological Reviews* 85: 361–392.
- 556 Kubo, T., Mitchell, M.T., and Henderson, D.M. 2012. *Albertonectes*  
557 *vanderveldei*, a new elasmosaur (Reptilia, Sauropterygia) from the Upper  
558 Cretaceous of Alberta. *Journal of Vertebrate Paleontology* 32: 557–572.

559 Lizuain, A., and Silva-Nieto, D., 1996, Estratigrafía mesozoica del río Chubut medio  
560 (Sierra de Taquetrén). Provincia de Chubut, *en* 13° Congreso Geológico Argentino  
561 y 3° Congreso de Exploración de Hidrocarburos (Buenos Aires), Actas 1: 479–493.

562 Massare, J. A., and Sperber, S.T. 2001. Vertebral morphology and swimming styles in  
563 Cretaceous plesiosaurs (Reptilia: Sauropterygia). *Paludicola* 3: 95–103.

564 O'Gorman, J.P. 2013. [ Plesiosaurios del Cretácico Superior de Patagonia y Península  
565 Antártica, Tomos I y II. PhD thesis, Facultad de Ciencias Naturales y Museo,  
566 Universidad Nacional de La Plata, Argentina. 527 p. Unpublished.].  
567 [http://sedici.unlp.edu.ar/bitstream/handle/10915/26140/Tomo\\_I\\_Documento](http://sedici.unlp.edu.ar/bitstream/handle/10915/26140/Tomo_I_Documento_completo.pdf?sequence=4)  
568 [completo.pdf?sequence=4](http://sedici.unlp.edu.ar/bitstream/handle/10915/26140/Tomo_I_Documento_completo.pdf?sequence=4)  
569 [http://sedici.unlp.edu.ar/bitstream/handle/10915/26140/Tomo\\_II\\_Documento](http://sedici.unlp.edu.ar/bitstream/handle/10915/26140/Tomo_II_Documento_completo.pdf?sequence=4)  
570 [completo.pdf?sequence=4](http://sedici.unlp.edu.ar/bitstream/handle/10915/26140/Tomo_II_Documento_completo.pdf?sequence=4)

571 O'Gorman, J.P., Gasparini, Z., and Salgado, L. 2013a. Postcranial morphology of  
572 *Aristonectes* Cabrera, 1941 (Plesiosauria, Elasmosauridae) from the Upper  
573 Cretaceous of Patagonia and Antarctica. *Antarctic Science* 25: 71–82

574 O'Gorman, J.P., Gasparini, Z., and Salgado, L. 2014a. Reappraisal of *Tuarangisaurus?*  
575 *cabazai* (Elasmosauridae, Plesiosauria) from the Upper Maastrichtian of northern  
576 Patagonia, Argentina. *Cretaceous Research* 47: 39–47.

577 O'Gorman, J.P., Otero, R.A., and Hiller, N. 2014b. A new record of an aristonectine  
578 elasmosaurid (Sauropterygia, Plesiosauria) from the Upper Cretaceous of New  
579 Zealand: implications for the *Mauisaurus haasti* Hector, 1874 hypodigm.  
580 *Alcheringa* 38: 504–512.

581 O'Gorman, J.P., Olivero, E.B., Santillana, S., and Everhart, M.J., and Reguero, M. 2014c.  
582 Gastroliths associated with an *Aristonectes* specimen (Plesiosauria,

583 Elasmosauridae), López de Bertodano Formation (upper Maastrichtian) Seymour  
584 Island (*Is. Marambio*), Antarctic Peninsula. *Cretaceous Research* 50: 228–237.

585 O’Gorman, J.P., Salgado, L., Olivero, E., and Marensi, S. 2015.. *Vegasaurus molyi* gen. et  
586 sp. nov. (Plesiosauria, Elasmosauridae) from the Cape Lamb Member (lower  
587 Maastrichtian) of the Snow Hill Island Formation, Vega Island, Antarctica, and  
588 remarks on Wedellian Elasmosauridae. *Journal of Vertebrate Paleontology* (DOI:  
589 [10.1080/02724634.2014.931285](https://doi.org/10.1080/02724634.2014.931285)).

590 Otero, R.A., Soto-Acuña, S., and Rubilar-Rogers, D. 2012. A postcranial skeleton of an  
591 elasmosaurid plesiosaur from the Maastrichtian of central Chile, with comments on  
592 the affinities of Late Cretaceous plesiosauroids from the Weddellian Biogeographic  
593 Province. *Cretaceous Research* 37: 89–99.

594 Otero, R.A., Soto-Acuña, S., O’Keefe, F.R., O’Gorman, J.P., Stinnesbeck, W. Suárez, M.A.,  
595 Rubilar-Rogers, D., Quinzio-Sinn, L.A., and Salazar, C. 2014. *Aristonectes*  
596 *quiriquinensis* sp. nov., a new highly derived elasmosaurid from the late  
597 Maastrichtian of central Chile 34: 100–125.

598 Otero R.A., and O’Gorman, J.P. 2013. Identification of the first postcranial skeleton of  
599 *Aristonectes* Cabrera (Plesiosauroidea, Elasmosauridae) from the upper  
600 Maastrichtian of the south-eastern Pacific, based on a bivariate graphic analysis.  
601 *Cretaceous Research* 41: 86–89.

602 O’Keefe, F.R., and Street, H.P. 2009. Osteology of the cryptocleidoid plesiosaur *Tatenectes*  
603 *laramiensis*, with comments on the taxonomic status of the Cimoliasauridae.  
604 *Journal of Vertebrate Paleontology* 29: 48–57.

605 Page, R., Ardolino, A., de Barrio, R.E., Franchi, M., Lizuain, A., Page, S., Silva Nieto,  
606 D., 1999. Estratigrafía del Jurásico y Cretácico del Macizo de Somún Curá,

607 provincias de Río Negro y Chubut. In: R. Caminos (Ed) *Geología Argentina*.  
608 SEGEMAR, Buenos Aires, p.460–488.

609 Lesta, P., and Ferello, R. 1972. Región Extrandina del Chubut y norte de Santa Cruz. In:  
610 A.F. Leanza (Ed.), *Geología Regional Argentina*. Academia Nacional de Ciencias  
611 de Córdoba, Córdoba, p.601–654.

612 Owen, R. 1860. On the orders of fossil and recent Reptilia, and their distribution in time.  
613 *Reports of the British Association for the Advancement of Science* 29: 153–166.

614 Persson, P.O. 1963. A Revision of the classification of the Plesiosauria with synopsis of the  
615 stratigraphical and geographical distribution of the group. *Lunds Universitets*  
616 *Årsskrift* 59: 1–60.

617 Sato, T. 2003. *Terminonator ponteixensis*, a new elasmosaur (Reptilia; Sauropterygia) from  
618 the Upper Cretaceous of Saskatchewan. *Journal of Vertebrate Paleontology* 23: 89–  
619 103.

620 Sachs, S., and Kear, B. P. 2014. Postcranium of the paradigm elasmosaurid plesiosaurian  
621 *Libonectes morgani* (Welles, 1949). *Geological Magazine*, 1–17.  
622 doi:10.1017/S0016756814000636.

623 Sato, T., Hasegawa, Y., and Manabe, M. 2006. A new elasmosaurid plesiosaur from the  
624 Upper Cretaceous of Fukushima, Japan. *Palaeontology* 49: 467–484.

625 Schumacher, B.A. 2008. On the skull of a pliosaur (Plesiosauria; Pliosauridae) from the  
626 Upper Cretaceous (early Turonian) of the North American Western  
627 Interior. *Transactions of the Kansas Academy of Science* 111: 203–218.

628 Schumacher, B.A., Carpenter, K., and Everhart, M.J. 2013. A new Cretaceous pliosaurid  
629 (Reptilia, Plesiosauria) from the Carlile Shale (Middle Turonian) of Russell County,  
630 Kansas. *Journal of Vertebrate Paleontology* 33: 613–628.

631 Vincent, P., Bardet, N., Suberbiola, X.P., Bouya, B., Amaghaz, M., and Meslough, S. 2011.  
632 *Zarafasaura oceanis*, a new elasmosaurid (Reptilia: Sauropterygia) from the  
633 Maastrichtian Phosphates of Morocco and the palaeobiogeography of latest  
634 Cretaceous plesiosaurs. *Gondwana Research* 19: 1062–1073.

635 Welles, S.P. 1943. Elasmosaurid plesiosaurs with description of new material from  
636 California and Colorado. *Memoirs of the University of California* 13: 125–234.

637 Welles, S.P. 1949. A new elasmosaur from the Eagle Ford Shale of Texas. Part I.  
638 Systematic description. *Fondren Science Series* 1: 1–28.

639 Welles, S.P. 1952. A Review of the North American Cretaceous Elasmosaurs. *University of*  
640 *California Publications in Geological Sciences* 29: 1–144.

641 Welles, S.P. 1962. A new species of Elasmosaur from the Aptian of Colombia and a review  
642 of the Cretaceous plesiosaurs. *University of California Publications in Geological*  
643 *Sciences* 44: 1–96.

644 Wiffen, J., and Moisley, W.L. 1986. Late Cretaceous reptiles (Families Elasmosauridae and  
645 Pliosauridae) from the Mangahouanga Stream, North Island, New Zealand. *New*  
646 *Zealand journal of geology and geophysics* 29: 205–252.

647 Williston, S.W. 1903. North American plesiosaurs, Part 1. Field Columbian Museum  
648 Publication (Geology) 73:1–77.

649 Zammit, M., Daniels, C.B., and Kear, B.P. 2008. Elasmosaur (Reptilia: Sauropterygia)  
650 neck flexibility: Implications for feeding strategies. *Comparative Biochemistry and*  
651 *Physiology Part A: Molecular & Integrative Physiology* 150: 124–130.

652  
653  
654

655 Figure captions

656 **Figure 1.** **1**, Original display of the holotype; **2**, artistic representation of *A. parvidens*  
657 made by Ángel Cabrera; **3**, approximate locality where the MLP 40-XI-14-6 (holotype of  
658 *A. parvidens*) was collected. Modified from Lizuaín and Silva-Nieto (1996).

659 **Figure 2.** *Aristonectes parvidens* holotype (MLP 40-XI-14-6). **1–2**, skull with plaster  
660 reconstruction in **1**, dorsal and **2**, ventral views. Scale bars= 40 mm. **3**, cranium and  
661 mandible in anterior view. Scale bar= 20 mm. **4**, cranium and mandible in right lateral  
662 view. Scale bar= 100 mm. **5**, posterior part of cranium and mandible. Scale bar= 20 mm. **6**,  
663 anterior part of cranium and mandible in anterior-right view showing alveoli disposition.  
664 Scale bar= 20 mm.

665 **Figure 3.** *Aristonectes parvidens* holotype (MLP 40-XI-14-6). **1**, cranium and mandible in  
666 ventral view. Scale bar= 100 mm. **2**, mandibular symphysis in posterior view, showing the  
667 “deep groove” of Otero *et al.*, (2014). **3–4**, anterior palate **3**, photo and **4**, interpretative  
668 drawing. Scale bar= 20mm. **5**, medial view of the middle and posterior part of the right  
669 mandible. Scale bar = 50 mm.

670 **Figure 4.** **1–4**, mandibular symphysis of elasmosaurids in ventral view. **1**, *Aristonectes*  
671 *parvidens* (MLP 40-XI-14-6). **2**, *Tuarangisaurus keyesi* (NZGS, CD425). **3**,  
672 *Callawayasaurus colombiensis* (UCMP 38349) and **4**, CIT 2749, referred to *Morenosaurus*  
673 *stocki* Welles, 1943. **5, 6**, quadrate and glenoyd cavity of *Aristonectes parvidens* (MLP 40-  
674 XI-14-6). Scale bar = 20mm.

675 **Figure 5.** *Aristonectes parvidens* comparative cranial and mandibular proportions and  
676 palatal structure. **1–2**, relative symphyseal length in ventra view **1**, *Aristonectes parvidens*,  
677 **2**, *Libonectes mogani*. **3–4**, relative symphyseal length in medial view **3**, *Aristonectes*  
678 *parvidens*, **4**, *Libonectes morgani*. Scale bar= 100 mm. **5–6**, relative premaxillar length in

679 palatal view **5**, *Aristonectes parvidens* **6**, *Libonectes morgani*. Not in scale. **7–10**,  
680 comparison of premaxilla anteroposterior lateral length **7**, *Kaiwhekea katiki* **8**, *Aristonectes*  
681 *parvidens* **9**, *Libonectes morgani* and **10**, *Terminonatator ponteixensis* Sato, 2003. **11–12**,  
682 palatal structures of **12**, *Aristonectes* and **11**, *Libonectes morgani*. Not in scale (**2**, **4**, **6**, **9**,  
683 modified from Carpenter, 1997; **7** modified from Cruickshank and Fordyce, 2002; **10**,  
684 modified from Sato, 2003).

685 **Figure 6.** Cranial and cervical feature of *A. parvidens*. **1**, relation between the cranium  
686 length and the accumulative cervical length. **2**, cranium lengths. Data taken from Weles,  
687 1943, 1952; Wiffen and Moysley, 1986; Cruickshank and Fordyce, 2002.

688 **Figure 7.** **1**, scheme indicating the mesodistal length measure of alveoli; **2**, alveolar  
689 mesodistal length of *A. parvidens* and *Tuarangisaurus keyesi*. **3**, BI measurement of the  
690 anterior cervical centra of *A. parvidens* and three non-aristonectine elasmosaurids. Data  
691 taken from Weles, 1943, 1952.

692 **Figure 8.** *Aristonectes parvidens* holotype (MLP 40-XI-14-6). **1–4** atlas-axis complex in **1**,  
693 left lateral, **2**, detail of axis neural spine, **3**, anterior, **4**, axis rib, **5**, posterior and **6**, ventral  
694 views. Scale bar= 20 mm.

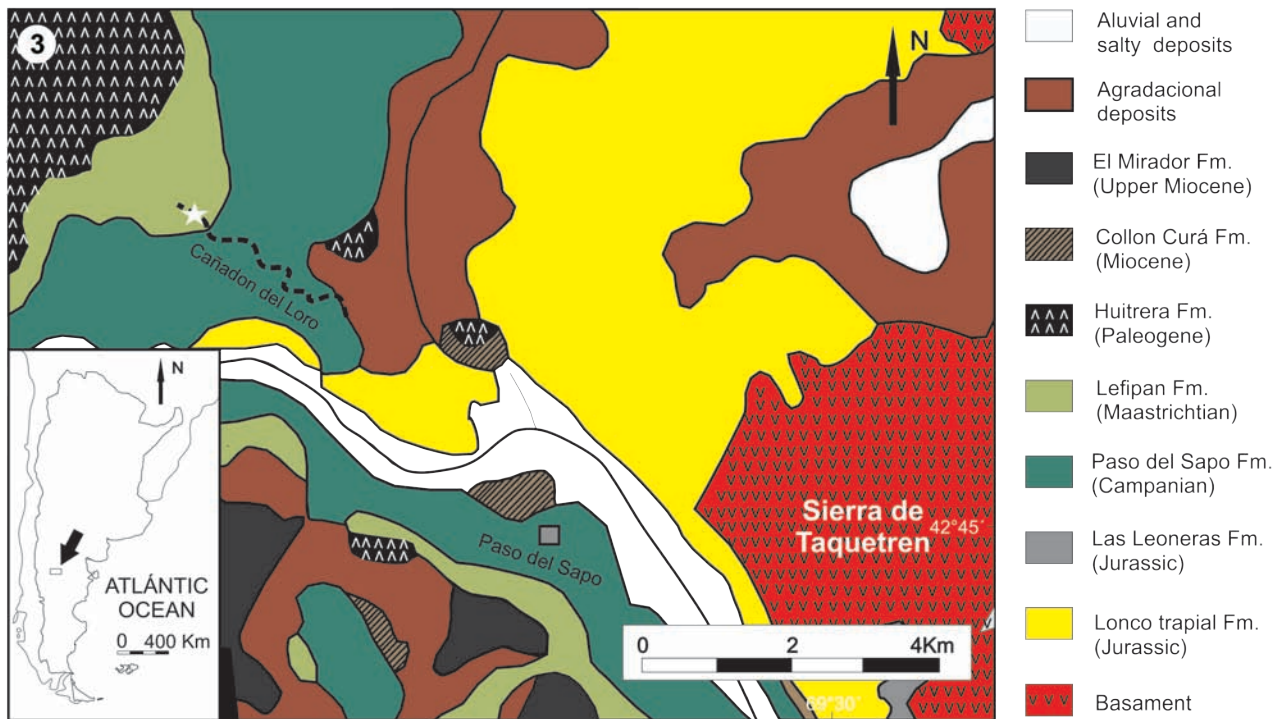
695 **Figure 9.** Atlas-axis complex of elasmosaurids. **1–2**, *Aristonectes parvidens* (holotype,  
696 MLP 40-XI-14-6) in **1**, anterior and **2**, ventral views. **3–4**, *Vegasaurus molyi* (holotype,  
697 MLP 93-I-5-1) in **5**, anterior and **6**, ventral views. **5–6**, *Tuarangisaurus keyesi* (holotype,  
698 NZGS, CD 426) in **5**, anterior and **6**, in ventral views. **7–8**, *Albertonectes vanderveldei*  
699 (holotype, TMP 2007.011.0001) in **7**, anterior and **8**, ventral views. Scale bar= 20 mm.

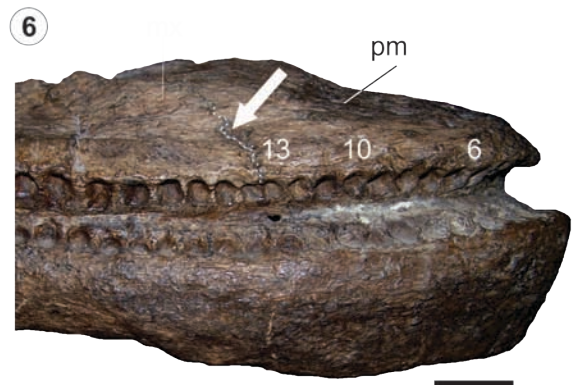
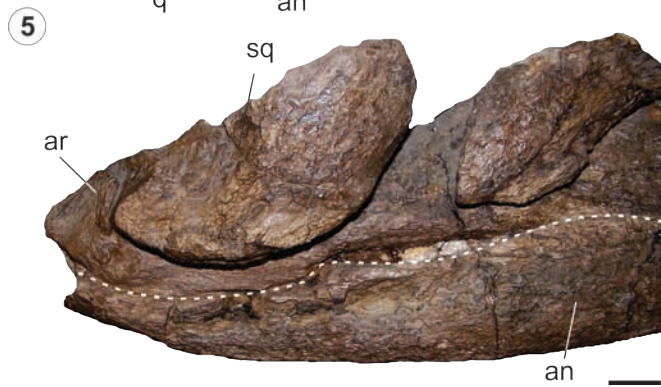
700 **Figure 10.** *Aristonectes parvidens* holotype (MLP 40-XI-14-6). **1**, sequence composed by  
701 3<sup>th</sup> to 19<sup>th</sup> cervical vertebrae. Scale bar = 100 mm. **2**, cervical vertebrae 11<sup>th</sup>–12<sup>th</sup> in left  
702 lateral view. **3**, 11<sup>th</sup> vertebrae in anterior view. **4**, 11<sup>th</sup>–12<sup>th</sup> vertebrae in ventral view. **5–6**,

703 9<sup>th</sup> cervical vertebrae in **5**, anterior view and **6**, reconstruction of cervical ribs in the 9<sup>th</sup>  
704 cervical vertebrae. **7**, 10<sup>th</sup> cervical vertebrae of *Vegasaurus molyi* (MLP 93-I-5-1) in  
705 posterior view. **8–9**, 17<sup>th</sup>–19<sup>th</sup> cervical vertebrae in **8**, left lateral and **9**, ventral view. **10**,  
706 cervical vertebrae of the non aristonectine *Afrosaurus furlongi* in left lateral view. Scale  
707 bars = 20 mm.

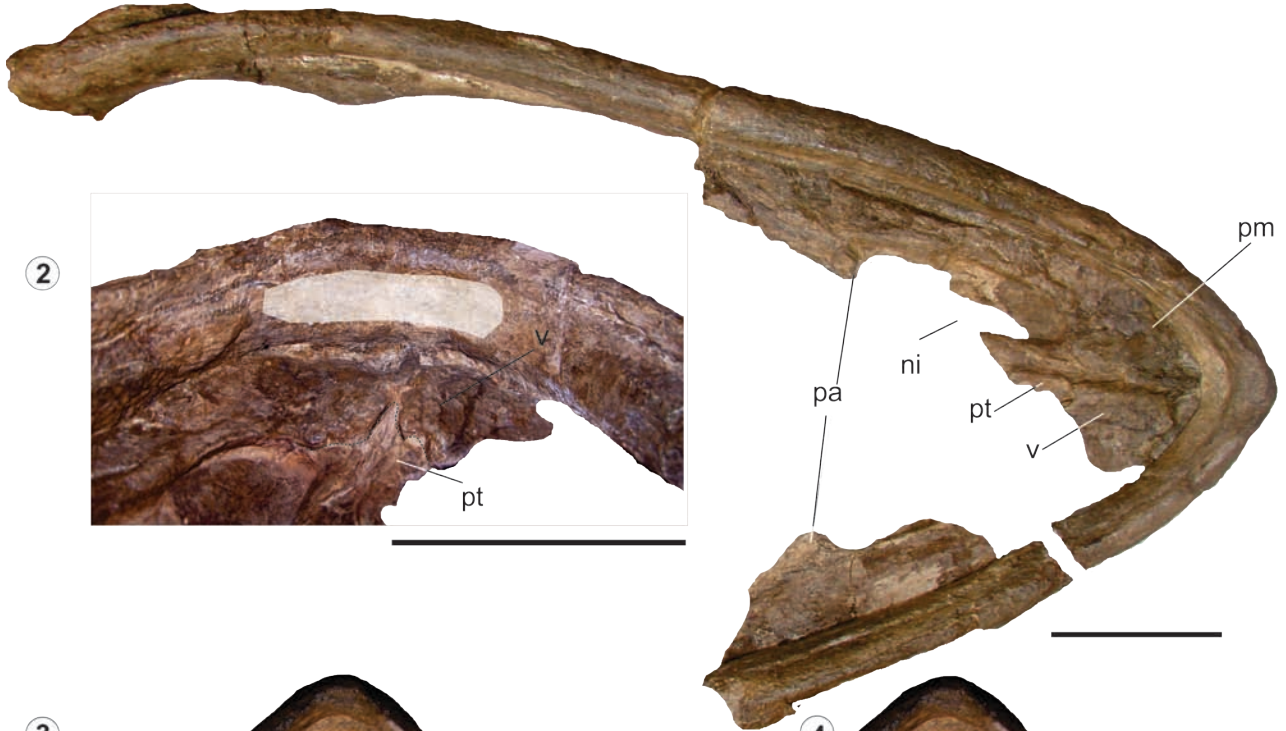
708 **Figure 11.** *Aristonectes parvidens* holotype (MLP 40-XI-14-6). **1–4** caudal centra in **1**,  
709 anterior; **2**, left lateral; **3**, ventral and **4**, dorsal views. **6–7**, caudal rib in **6**, posterior? and **7**,  
710 dorsal? views. **8–9**, posterior? limb **8**, original display and **9**, reconstruction. Scale bars =  
711 40 mm. **10**, plot of the HI and BI index of the caudal vertebrae of MLP 40-XI-14-6 and non  
712 aristonectine elasmosaurids.







1



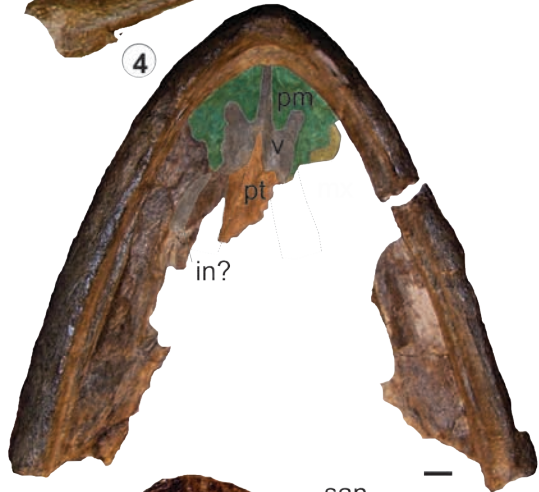
2



3



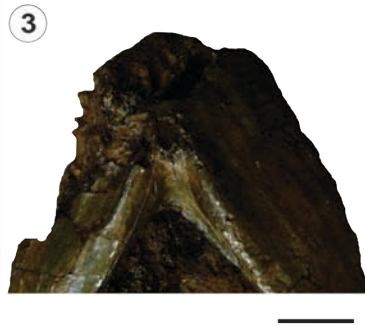
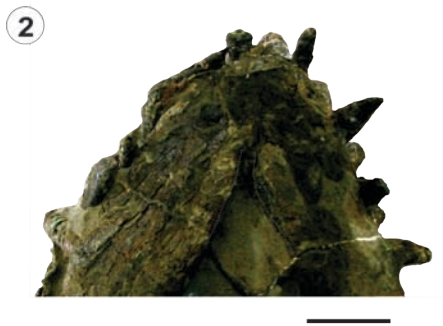
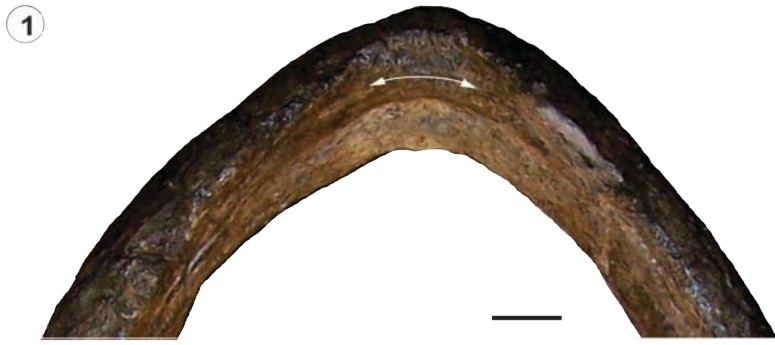
4

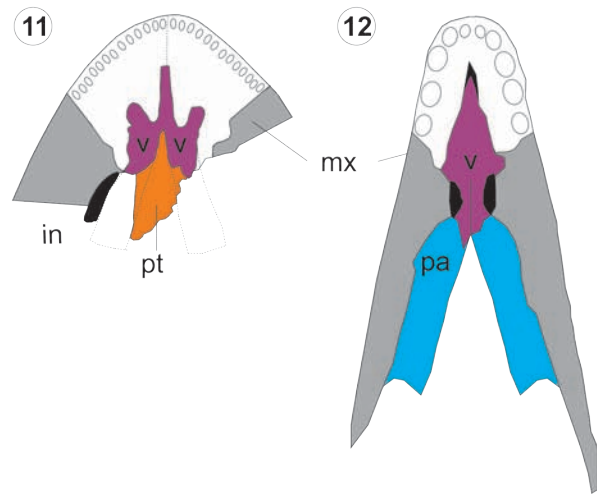
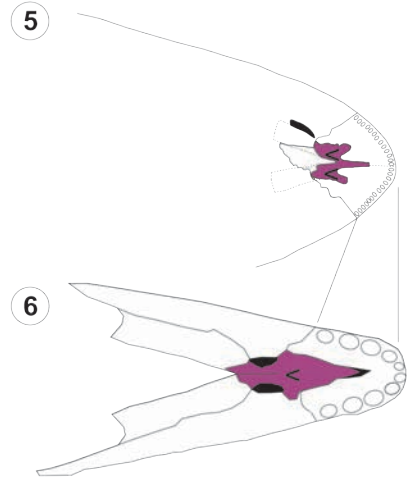
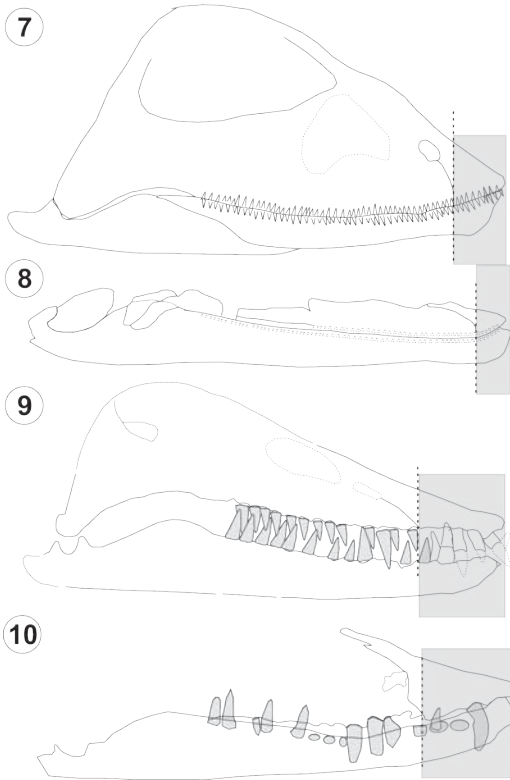
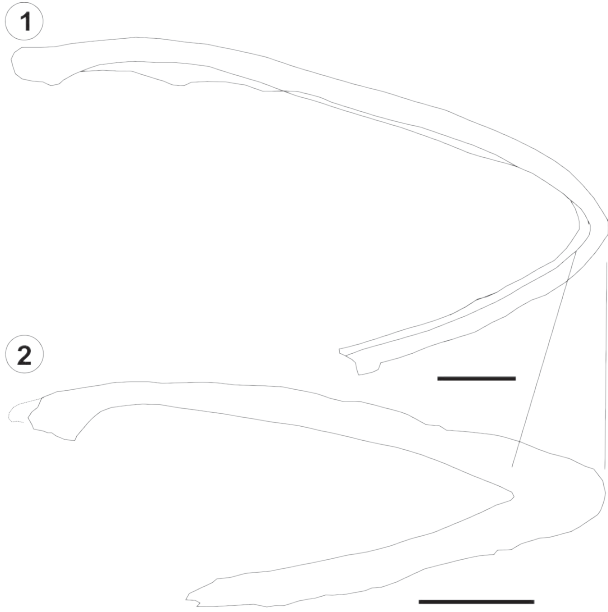


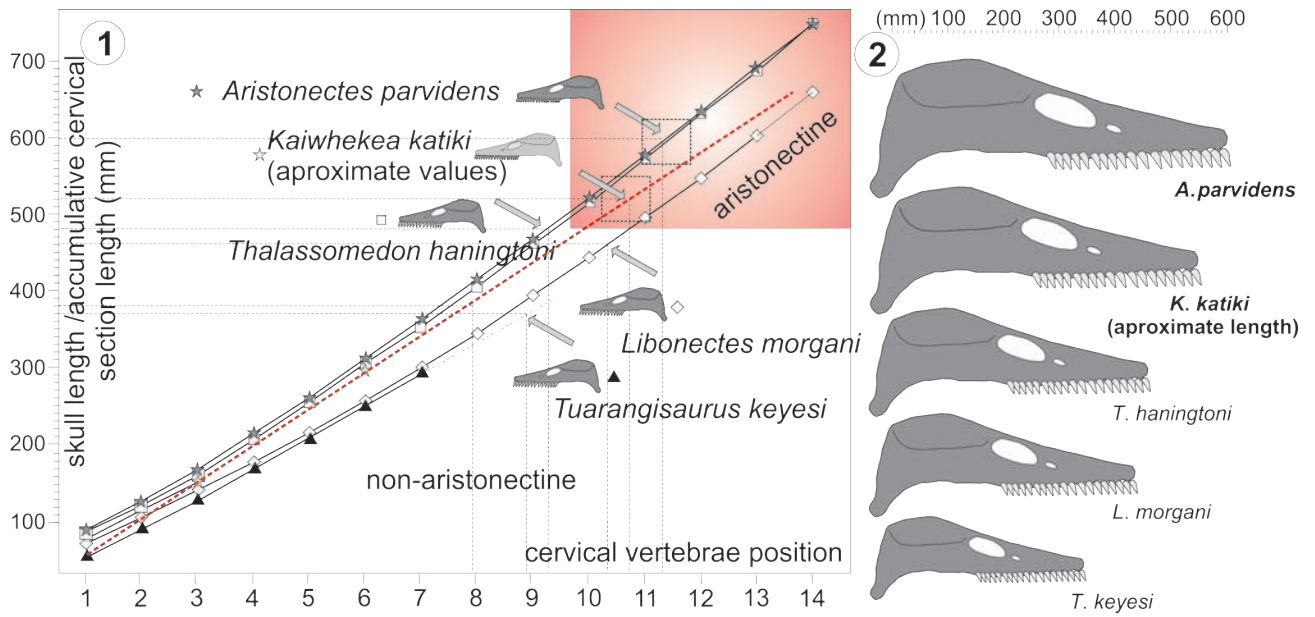
5

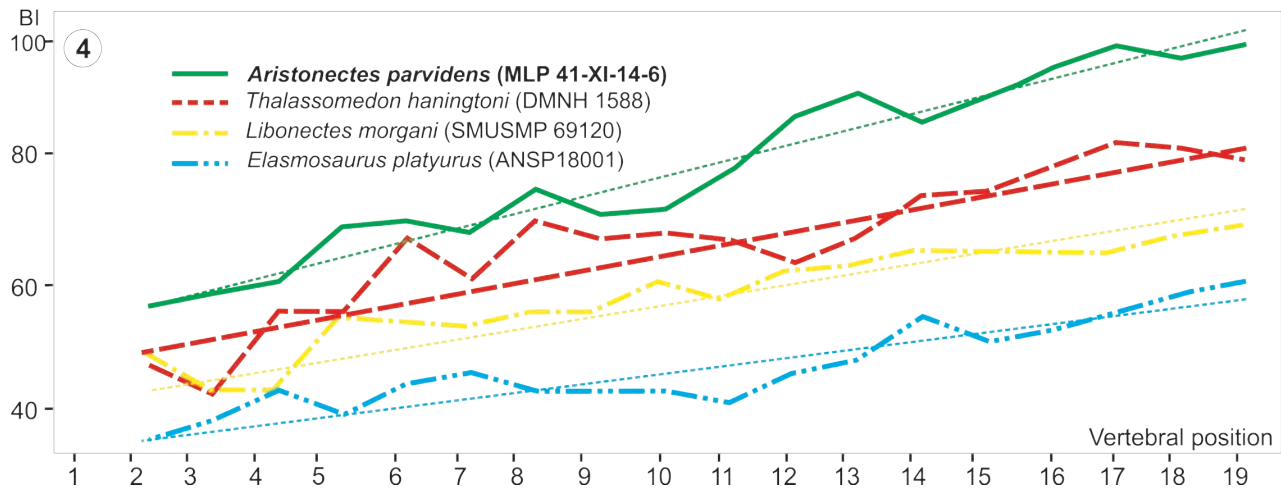
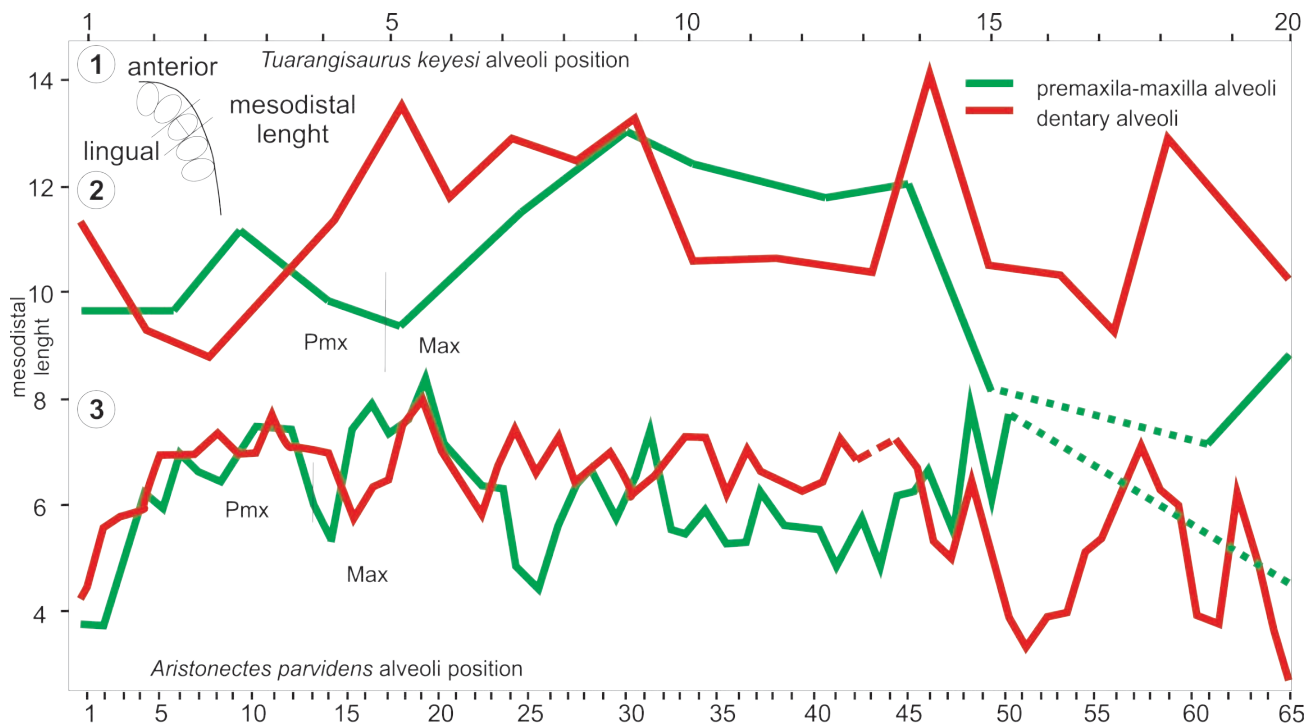






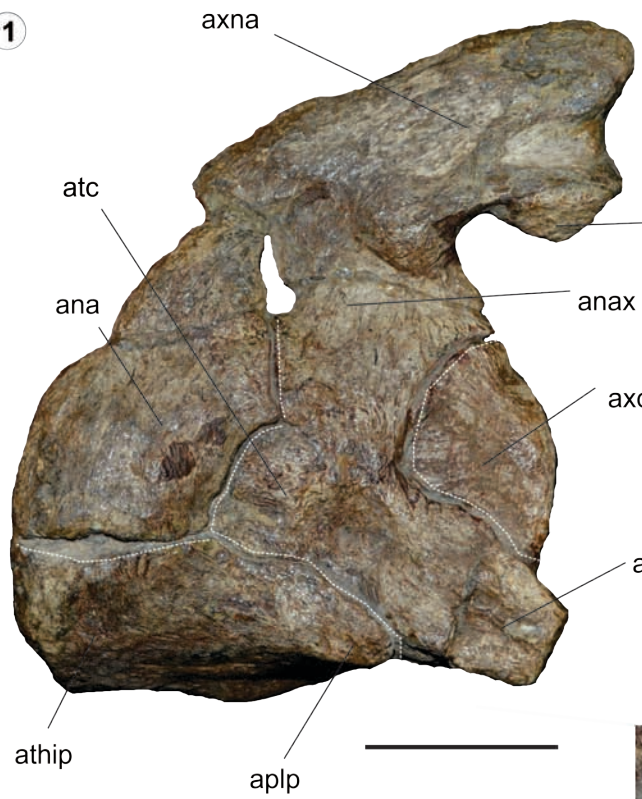




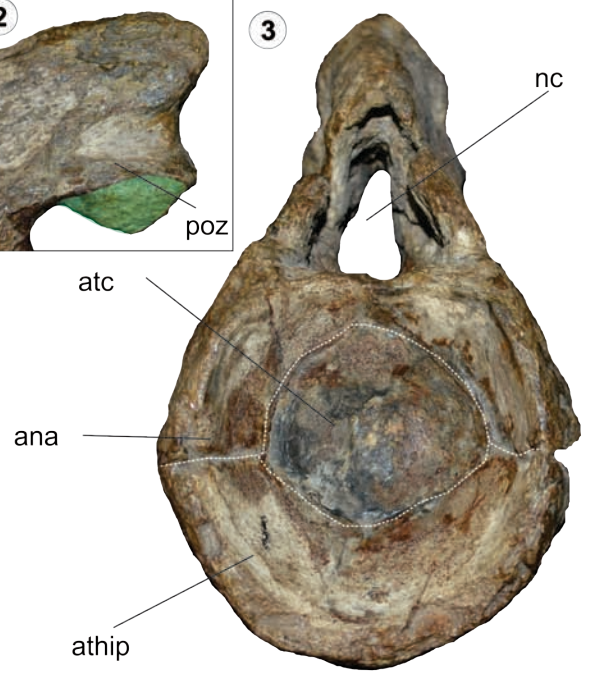




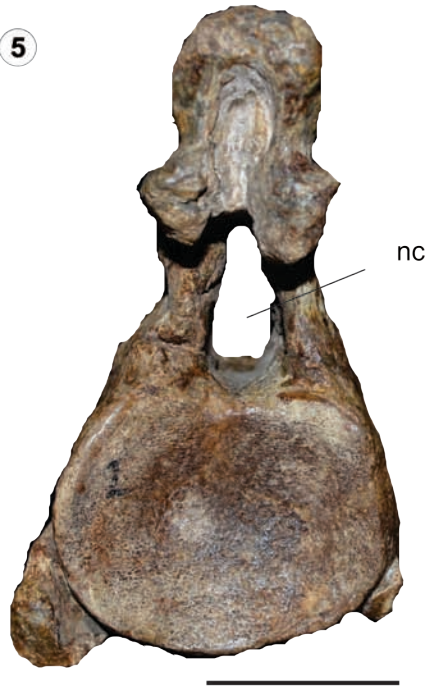
1



3



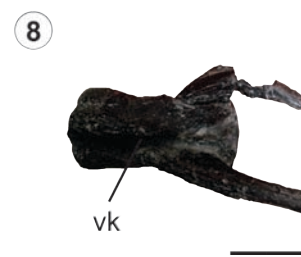
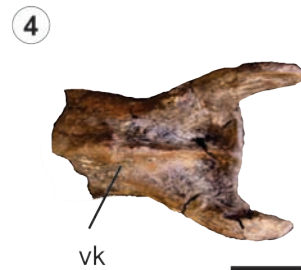
5

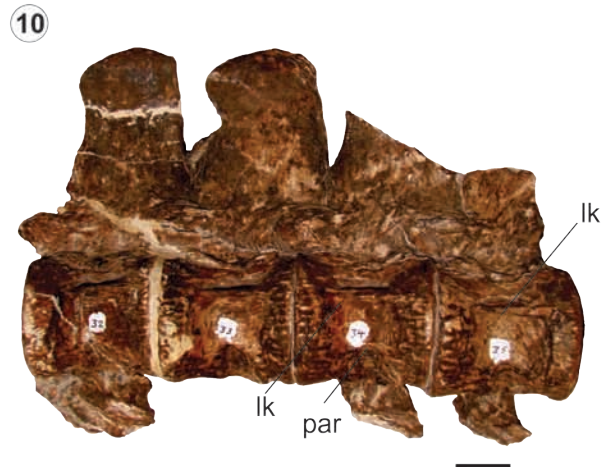
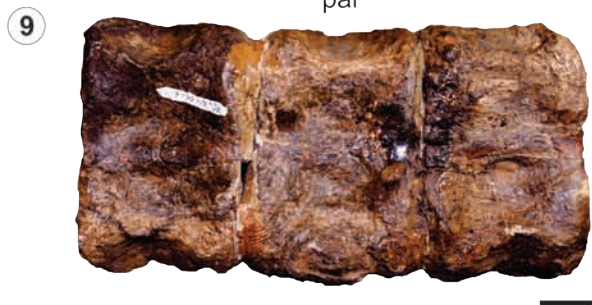
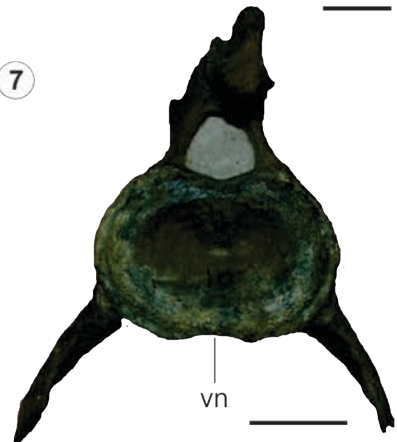
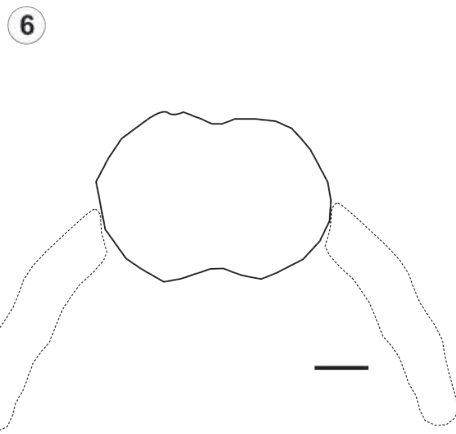


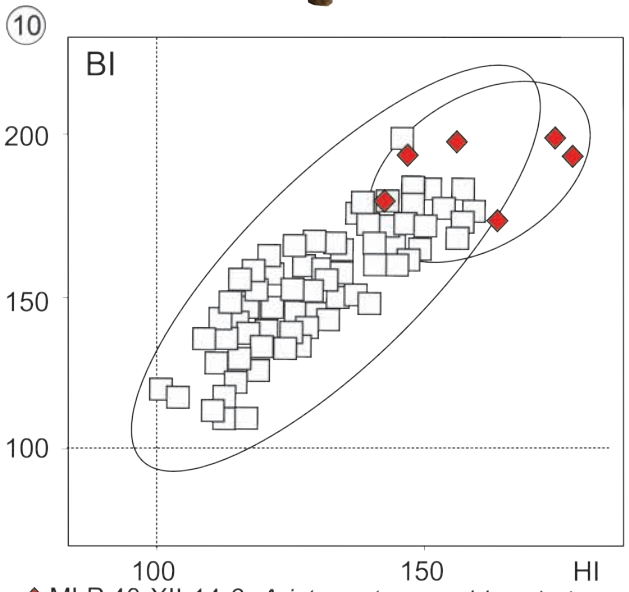
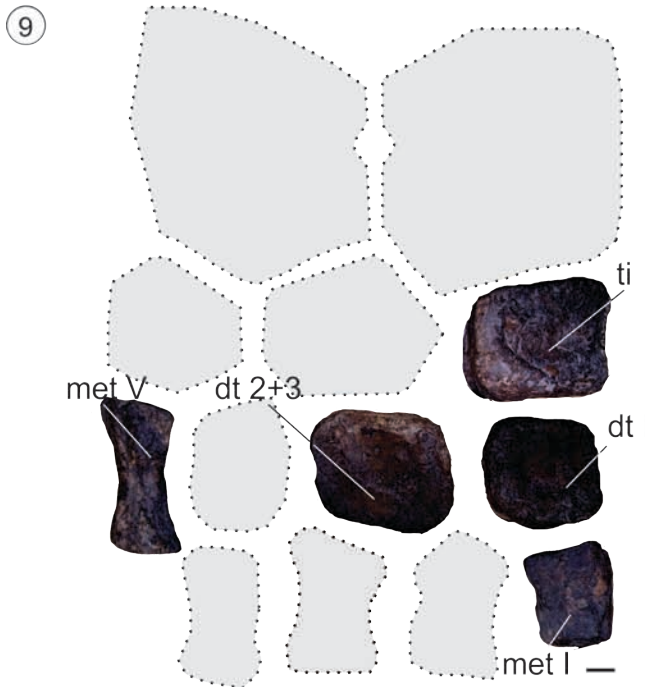
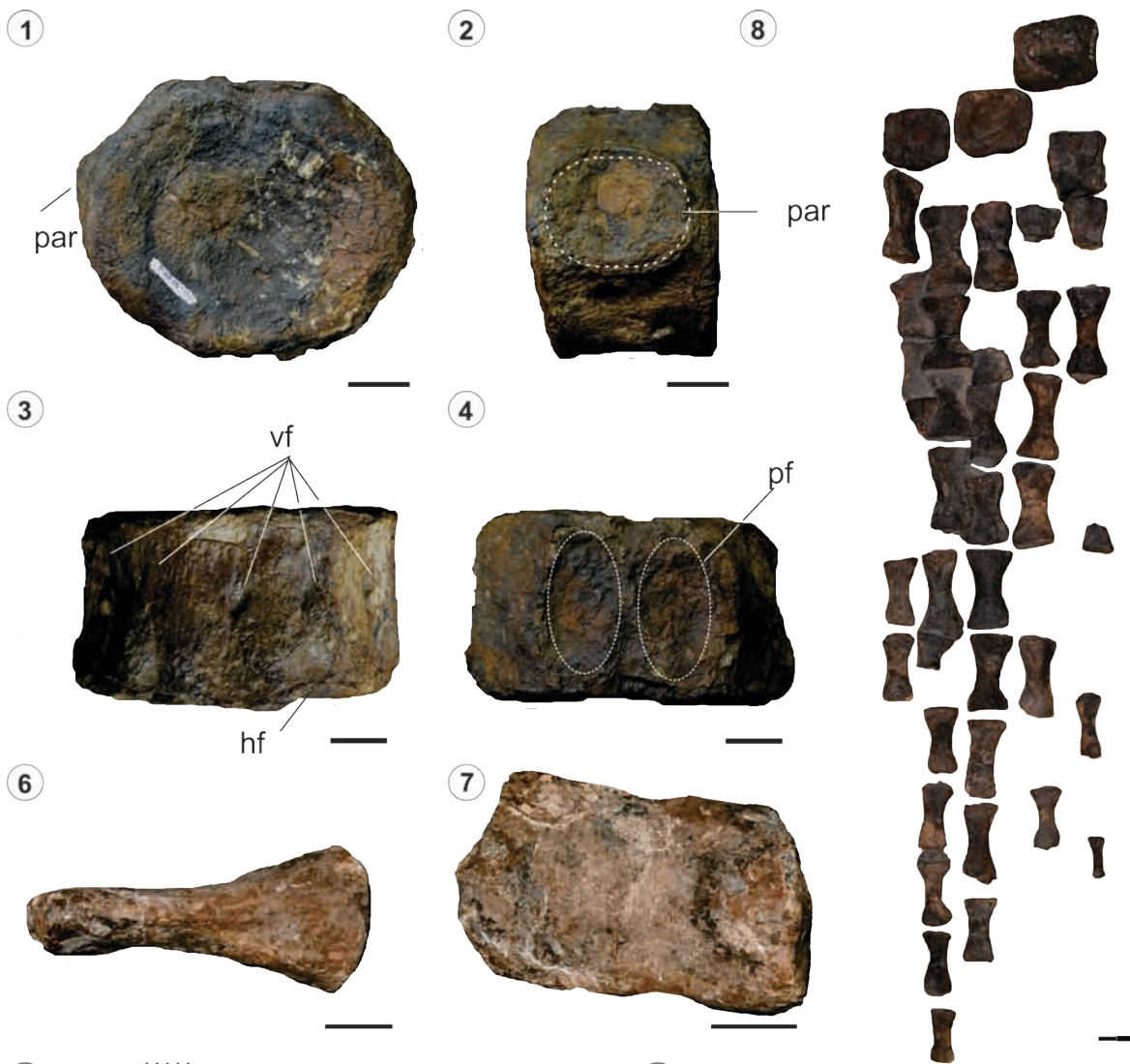
6











◆ MLP 40-XII-14-6. *Aristonectes parvidens* holotype  
 ■ MLP 71-II-13-1; MUC Pv 92 Elasmosauridae indet.  
 ANSP N° 10081 *Elasmosaurus platyurus*;  
 DMNH N° 1588 *Thalassomedon haningtoni*  
 MML PV 4 (Elasmosauridae indet.)

**TABLE 1- Elasmosaurid taxa considered on the quantitative comparison with *Aristonectes parvidens*. Data taken from (Cabrera, 1941; Welles, 1943; Wiffen and Moysley, 1986; Carpenter, 1999; Cruickshank and Fordyce, 2002; Sach and Kear, 2014).**

Taxa	Specimen	Locality/stratigraphy
<b><i>Thalassomedon haningtoni</i></b> Welles, 1943	UNSM 50132	Baca County, Colorado, USA/ Graneros Shale, lower Cenomanian
<b><i>Tuarangisaurus keyesi</i></b> Wiffen and Moysley, 1986	NZGS, CD425	Mangahouanga Stream, inland Hawke's Bay, New Zealand/ Tahora Formation. upper Campanian-lower Maastrichtian
<b><i>Callawayasaurus colombiensis</i></b> (Welles) Carpenter, 1999	UCMP 38349	Villa de Leyva, Colombia/Paja Fm. upper Aptian
<b><i>Libonectes morgani</i></b> Welles, 1949	MU SMP 69120	Dallas County, Texas, USA/ Britton Fm. upper Cenomanian
<b><i>Aristonectes parvidens</i></b> Cabrera, 1941	MLP 40-XI-14-6	Paso del Sapo, CUBUT Province, Argentina/Lefipan Fm. Maastrichtian.
<b><i>Kaiwhekea katiki</i></b> Cruickshank and Fordyce, 2002	OU 12649	Shag Point, North Otago, New Zealand. Katiki Fm. boundary between Upper and Lower Maastrichtian

**TABLE 2-Aristonectes parvidens MLP 40-XI-14-6, cranium and mandible measurements (in mm). ~ indicates approximate measurements.**

<i>Measurement</i>	<i>value (mm)</i>
<i>skull length</i>	<i>~600</i>
<i>pre-glenoid length</i>	<i>674</i>
<i>premaxilla anteroposteriorly length</i>	<i>74</i>
<i>premaxilla transversely length</i>	<i>135</i>
<i>symphysis anterioposterior length</i>	<i>45.33</i>
<i>mandible height at coronoid process level</i>	<i>124</i>
<i>coronoid-symphysis distance</i>	<i>534</i>

**TABLE 3- *Aristonectes parvidens* MLP 40-XI-14-6 vertebral measurements (in mm): L, length; H, height and B, breadth, indexes HI, height (H)/length (L) ratio ( $HI=100*H/L$ ), BI, breadth (B)/length (L) ratio ( $BI=100*B/L$ ), BHI, breadth/height ratio ( $BHI=100*B/H$ ) and VLI, Vertebral Length Index [ $VLI= 100*L / (0.5*(H + B))$ ].**

<i>Cervical vertebrae</i>	<i>L</i>	<i>H</i>	<i>B</i>	<i>HI</i>	<i>BI</i>	<i>BHI</i>	<i>VLI</i>
1+2	82	43	56	52	68	130	-
3	40	45	58	113	145	129	78
4	44	49	60	111	136	122	81
5	46	51	69	111	150	135	77
6	49	55	70	112	143	127	78
7	52	50	68	96	131	136	88
8	51	55	75	108	147	136	78
9	52	55	71	106	137	129	83
10	52	54	72	104	138	133	83
11	55	55	78	100	142	142	83
12	56	56	87	100	155	155	78
13	56	60	91	107	163	152	74
14	56	57	86	102	154	151	78
15	55	60	90	109	164	150	73
16	68	68	95	100	140	140	83
17	58	62	99	107	171	160	72
18	63	62	97	98	154	156	79
19	63	64	99	102	157	155	77
<i>Caudal vertebrae</i>							
1	71	-	-	-	-	-	-
2	70	110	121	157	173	110	61
3	70	99	121	141	173	122	64
4	63	-	-	-	-	-	-
5	58	97	116	167	200	120	54
6	66	89	118	135	179	133	64
7	61	91	121	149	198	133	58
8	65	91	127	140	195	140	60
9	55	77	98	140	178	127	63

**TABLE 4- Number of dentary alveoli (Al), skull length (SL, in mm), and ratio between both values (Ar) and the predicted number of aristonectine alveoli number based on a non elasmosaurid mandible sizes. Values in italics are approximate. For calculation Tuarangisaurus (20 alveoli); Aristonectes (64 alveoli) and Kaiweheka (43 alveoli) were considered. Data taken from (Welles, 1943, 1962; Wiffen and Moislely, 1986; Carpenter, 1999; Cruickshank and Fordyce, 2002; Sato, 2002; J.P.O'G. pers. obs).**

<i>Taxon</i>	<i>Dentary alveoli (Al)</i>	<i>Skull length (SL)</i>	<i>AR= SL/Al</i>	<i>Predicted alveoli number</i>	
				<b>Aristonectes (63-65)</b>	<b>Kaiweheka (42-44)</b>
<b>Callawayasaurus</b> ( <i>UCMP 38349</i> )	20	350	0.05714	34	30
<b>Thalassomedon</b> ( <i>UNSM 50132</i> )	17	480	0.03541	21	18
<b>Tuarangisaurus</b> ( <i>NZGS, CD425</i> )	19-21	370	0.05405	32	28
<b>Libonectes</b> ( <i>SMU SMP 69120</i> )	18	466	0.03862	23	20
<b>Aristonectes</b> ( <i>MLP 40-XI-14-6</i> )	63-65	600	0.10416		
<b>Kaiweheka</b> ( <i>OU 12649</i> )	42-44	520	0.08269		



**TABLE 5- Indicates the ratio between skull length and atlas axis length in aristonectine and non-aristonectine elasmosaurids. Values in bold are approximate. Data taken from (Welles, 1943, 1962; Wiffen and Moisley, 1986; Carpenter, 1999; J.P.O'G pers Obs.).**

<i>Taxon</i>	<i>Skull length (mm)</i>	<i>Atlas-axis complex length (mm)</i>	<i>Ratio skull length/atlas axis length</i>
<b>Thalassomedon haningtoni</b> (UNSM 50132)	480 mm	77	6.23
<b>Tuarangisaurus keyesi</b> (NZGS CD425)	370 mm	55	6.72
<b>Libonectes morgani</b> (SMU SMP 69120)	466 mm	60.3	7.72
<b>Aristonectes parvidens</b> (MLP 40-XI-14-6)	<b>600 mm</b>	82	7.31